

## Chemical Contrast in Soft X-Ray Ptychography

Mike Beckers,<sup>1,\*</sup> Tobias Senkbeil,<sup>1</sup> Thomas Gorniak,<sup>1</sup> Michael Reese,<sup>2</sup> Klaus Giewekemeyer,<sup>3</sup> Sophie-Charlotte Gleber,<sup>4</sup> Tim Salditt,<sup>3</sup> and Axel Rosenhahn<sup>1,5,†</sup>

<sup>1</sup>*Applied Physical Chemistry, Ruprecht-Karls-University Heidelberg, Im Neuenheimer Feld 253, 69120 Heidelberg, Germany*

<sup>2</sup>*Laser-Laboratorium Göttingen, Hans-Adolf-Krebs-Weg 1, 37077 Göttingen, Germany*

<sup>3</sup>*Institute for X-Ray Physics, Georg-August-University Göttingen, Friedrich-Hund-Platz 1, 37077 Göttingen*

<sup>4</sup>*X-Ray Science Division, Argonne National Laboratory, 9700 South Cass Avenue, Argonne Illinois 60439, USA*

<sup>5</sup>*Institute of Functional Interfaces, IFG, Karlsruhe Institute of Technology, PO Box 3640, 76021 Karlsruhe, Germany*

(Received 25 May 2011; published 8 November 2011)

The unique strengths of x-ray microscopy are high penetration depth and near-edge resonances that provide chemical information. We use ptychography, a coherent diffractive imaging technique that dispenses of the requirement for isolated specimens, and demonstrate resonant imaging by exploiting resonances near the oxygen *K* edge to differentiate between two oxygen-containing materials. To highlight a biological system where resonant ptychography might be used for chemical mapping of unsliced cells, reconstructions of freeze-dried *Deinococcus radiodurans* cells at an energy of 517 eV are shown.

DOI: 10.1103/PhysRevLett.107.208101

PACS numbers: 87.59.-e, 42.30.Rx, 78.70.Dm

Because of their ability to penetrate matter, x rays allow high-resolution imaging of whole, unsliced cells, i.e., samples which are too thick for electron microscopy. Sudden changes in the photon absorption cross section at elemental absorption edges also provide chemical sensitivity. Especially in the water window, at photon energies between the *K* absorption edges of carbon and oxygen, biological specimens in their natural aqueous environment can be imaged with high contrast [1]. Experimental complications introduced by x-ray lenses (e.g., photon absorption in optical elements and loss of contrast) can be overcome if they are discarded and iterative algorithms are used to restore real-space object information from recorded (oversampled) diffraction patterns [2,3]. This, however, shifts problems from the experimental setup to the computational side, where sampling requirements do also have experimental implications.

Importantly, this approach of coherent diffractive imaging (CDI) is able to extract phase and amplitude properties of the sample from a single data set. Since many specimens, in particular, biological samples, may not absorb strongly but apportion much of their interaction with x rays to phase changes, information about both the real and imaginary part of the local complex refractive index provides essential knowledge about a sample. The first CDI phase retrieval algorithms required the specimen to be sufficiently well isolated [4–6], which impedes imaging of many biological samples like tissues and other extended objects. Imaging of extended samples which are not compactly supported became possible after introducing algorithms based on the overlap constraint [7,8], on multiple, overlapping positions of the sample in the known and illuminating x-ray beam.

More recently, a ptychographic algorithm was introduced [9] which allows us to retrieve both the complex

object and the (initially unknown) complex illumination function at the same time. This algorithm has since proven its applicability to visible light [10] and as a promising x-ray technique [9,11–15], allowing reconstructions of strongly and weakly scattering samples.

The increasing availability of high-brilliance synchrotron radiation sources has made x-ray imaging appealing to more and more applications, including chemical mapping of samples using a combination of near-edge x-ray-absorption fine structure spectroscopy (NEXAFS) and x-ray microscopy techniques [16–19] and element specific resonant imaging [20] with conventional x-ray diffraction microscopy.

Here we report on a previously undemonstrated application of ptychography to distinguish and spatially resolve two oxygen-containing materials, polymethylmethacrylate (PMMA) and silicon dioxide (SiO<sub>2</sub>), at different photon energies based on their photon absorption cross section differences in NEXAFS spectra near the oxygen *K* edge. We demonstrate that ptychography can provide chemical resolution in heterogeneous specimens, with both absorption and phase as possible contrast mechanisms.

Experiments were realized at the Berlin electron storage ring BESSY II at the undulator beam lines U49/2-PGM1 and UE52-SGM. For ptychographic imaging, the incident beam impinged on pinholes which were drilled by focused ion beam milling in gold foils of 1.86 μm thickness. The gold foils were previously evaporated onto Si<sub>3</sub>N<sub>4</sub> membranes using chromium as adhesion promoter. The x-rays passing through the pinhole were scattered at samples placed 0.7–1 mm behind the aperture. The resulting diffraction images were recorded using a CCD detector (back-illuminated Andor DX436, 2048 × 2048 pixels, 13.5 μm pixel size, Peltier cooled to –60 °C), placed 18 cm (U49/2-PGM1) or 28 cm (UE52-SGM) downstream

from the sample plane. Next to the CCD chip a photodiode has been mounted which can be moved into the beam to record transmission spectra of dedicated spectroscopy samples.

As a model system for chemical contrast in mixed-compound samples, we exploited spectral differences of PMMA and SiO<sub>2</sub> near the oxygen *K* edge. The carbonyl group in PMMA shows a prominent C = O peak at about 531.5 eV [21] that can be used to distinguish PMMA from SiO<sub>2</sub>, which does not show significant preedge absorption changes [22]. To achieve a sufficiently thin and homogeneous spectroscopy sample, a 1 μm thick layer of PMMA was spun cast onto a 100 nm Si<sub>3</sub>N<sub>4</sub> membrane. A transmission spectrum was recorded between 520.0 and 545.0 eV with a step size of 0.1 eV, by remotely tuning the beam line's grazing incidence monochromator. For every energy position the photocurrent was measured. A complete spectrum was recorded in less than 15 min, while a similar scan without any sample between aperture and photodiode was used for normalization. This measurement was performed at beam line UE52-SGM immediately prior to ptychographic scanning, to determine the precise energies for the resonant experiment. The x-ray absorption behavior of a material, described by the imaginary part of the complex refractive index usually written as  $n_c(E) = 1 - \delta(E) - i\beta(E)$ , is easily accessible through transmission measurements. However, light absorption and dispersion are coupled, and the real-part dependent phase shift  $\delta$  can be connected to the extinction coefficient  $\beta$  through the Kramers-Kronig relations, which reflect that the real and imaginary parts of a complex response function of a linear, causal system are linked as Hilbert transform pairs. To numerically calculate the dispersion spectrum of PMMA, Hilbert transforms were applied to the recorded data.

PMMA and SiO<sub>2</sub> particles with a diameter of 2 μm used as objects for resonant imaging were prepared by dispersing a mixture of microspheres in purified water onto a 50 nm Si<sub>3</sub>N<sub>4</sub> membrane and subsequent air drying. An isolated group of nine beads consisting of five PMMA and four SiO<sub>2</sub> beads was scanned at 18 × 15 (h × v) positions, with one illumination per position. We used a 2 μm pinhole and a scanning step size of 800 nm. Five scans were performed: one at the absorption maximum measured at 532.0 eV, two at surrounding near-baseline energies (530.8 and 533.4 eV), and two more at the greatest slopes of the C = O peak, corresponding to the energies where the smallest and largest phase shifts were expected (531.5 and 532.6 eV). All reconstructions were obtained using the algorithm introduced in [9]. The innermost 512 × 512 pixels of the diffraction images [Fig. 1(a)] were binned by a factor of 2 and evaluated, corresponding to a pixel size in the object plane of 96 nm. Figure 1(b) shows the reconstruction of the illumination function at 530.8 eV after 210 iterations and back propagation of the wave field

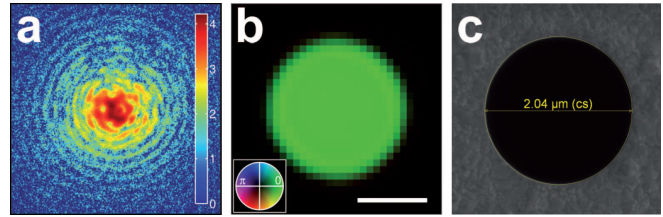


FIG. 1 (color online). (a) Central 512 × 512 pixels of one of the 270 diffraction patterns at 530.8 eV (logarithmic intensity scale) used in the ptychographic reconstruction. (b) Backpropagation of the reconstructed wave field at 530.8 eV into the exit plane of the aperture over a distance of 0.68 mm. The scale bar indicates a length of 1 μm. (c) SEM image of the 2 μm pinhole (downstream side).

into the plane of the aperture. It corresponds well to a scanning electron microscopy (SEM) image of the pinhole [Fig. 1(c)].

Whenever matter shows a strong interaction with the incoming beam, which is especially the case in the soft x-ray range, reconstructions may display unphysical phase jumps in regions where phase changes  $> \pi$  are induced by the specimen. Such discontinuities can be corrected by applying unwrapping routines to the phase reconstructions [12]. Reconstructions of amplitude and (unwrapped) phase of the five recorded ptychographic data sets are shown in Fig. 2 and compared to the changes in absorption and phase expected from spectroscopy data of PMMA. An estimate of the spatial resolution in the reconstructions is provided by comparing a line scan across the amplitude and phase reconstruction of a bead to the convolution of the expected amplitude and phase distribution, respectively, of a spherical particle with a Gaussian point spread function (PSF) [Fig. 2 inset]. If two PSFs with a full width half maximum (FWHM) of 0.5 and 1.5 image pixels are compared to the line scan profiles, a resolution in the range of one pixel (96 nm) seems reasonable. For the SiO<sub>2</sub> beads, the reconstructions of the complex object function show no significant change in absorption. A monotonic decrease of the phase shift is observed with increasing energy from 530.8 to 533.4 eV. This phase behavior corresponds to the large changes in  $\delta$  theoretically expected near the absorption edge. Because of preedge resonances, PMMA shows a completely different absorption and dispersion behavior in the same energy range. The phase reconstruction at 532.0 eV reveals a high noise level in regions where the beam is absorbed strongly by PMMA, with low photon transmission providing insufficient information about these regions during reconstruction. The absorption and phase shift in the ptychographic reconstructions correspond to the experimental absorption spectra and the calculated phase shift of PMMA. Obviously, the difference is large enough for easy discrimination of PMMA from SiO<sub>2</sub>. Note that through the availability of phase information in ptychography, chemical compounds of one element can be

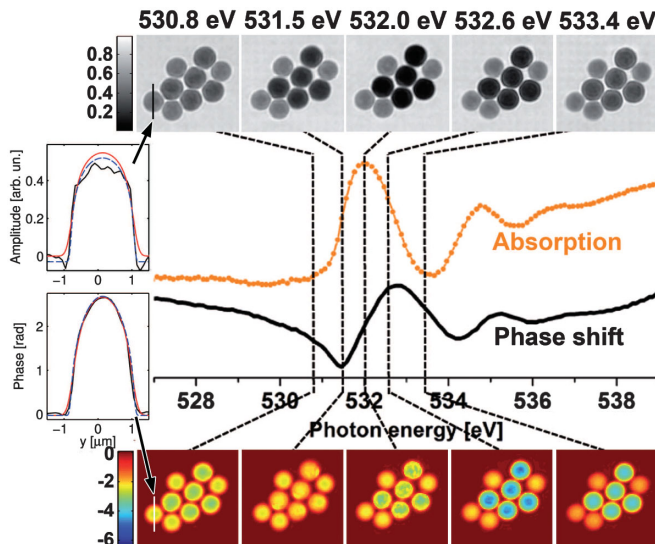


FIG. 2 (color). Reconstructions of amplitude and unwrapped phase (in radians) of five ptychographic data sets recorded at different energies around the measured C = O absorption peak of PMMA. The sample, a mixture of five PMMA beads and four SiO<sub>2</sub> beads each 2 μm in size, shows absorption and phase shift behavior that allows for easy discrimination of the two chemical compounds, corresponding to the experimental absorption spectrum and the calculated phase shift of PMMA. Inset: Resolution estimation via a line scan profile across amplitude and phase reconstruction of a bead (black curve), compared to the convolution of the thickness function of a 2 μm sphere and Gaussian point spread functions with FWHMs of 0.5 pixels (red curve) and 1.5 pixels (blue, dashed curve).

discriminated even when absorption images show similar contrast at different energies. In our case, this effect is especially striking at 531.5 and 532.6 eV, where PMMA can be distinguished from SiO<sub>2</sub> through a phase shift difference of PMMA of about 2.5 radians between both energies, while the SiO<sub>2</sub> beads, despite their same approximate thickness, show only a phase change of about 0.3 radians.

As the presented resonant imaging experiment can be interesting for chemically resolved imaging in biological applications, freeze-dried *Deinococcus radiodurans* cells were used for ptychography. *D. radiodurans* are bacteria which became famous due to their unusually high (and eponymous) resistance to ionizing radiation. Mechanisms leading to this resistance might be associated with the specific way the DNA is compacted and thus stabilized, or the accumulation of protective manganese complexes [23,24]. To demonstrate ptychography as an imaging method that in the future may help elucidate morphological and other factors contributing to this radioresistance, *D. radiodurans* cells have already been successfully subjected to ptychographic imaging in the hard x-ray regime at 6.2 keV, with low absorption preventing reconstruction of the real-valued amplitude, and phase shifts being of the

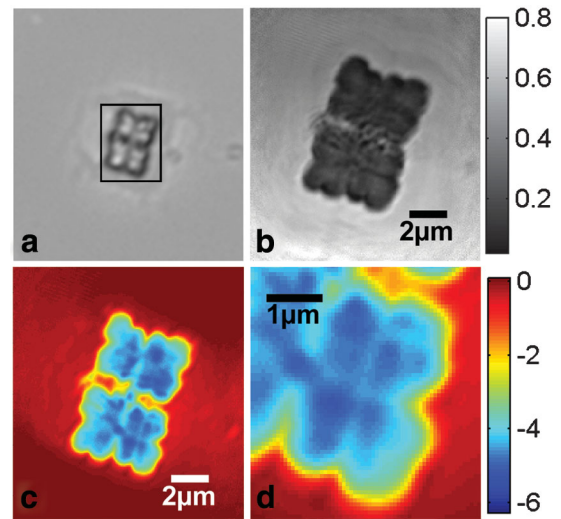


FIG. 3 (color). *D. radiodurans* cells. (a) Bright field microscopy image of a part of the specimen. Marked is the area of the ptychographic scan used for reconstruction. (b) Reconstructed amplitude of the cells. (c) Unwrapped phase shift of the cells and (d) detailed view.

order of 0.3 radians [14]. In the soft x-ray regime, absorption and phase shift can be expected to be much greater, alleviating ptychographic reconstruction of the complex object function. A sample consisting of freeze-dried *D. radiodurans* cells on a Si<sub>3</sub>N<sub>4</sub> membrane was scanned at 517 eV at 22 × 24 positions, using a 1 μm pinhole and a step size of 600 nm. This data set was acquired in about 60 min (dominated by detector readout), with a total exposure time to x rays of 79 s. A subsection of 15 × 19 positions was selected for reconstruction with 2000 iterations. Figure 3 shows amplitude and phase of the obtained complex-valued object function. The general appearance is consistent with the optical microscopy picture [Fig. 3(a)]. The cells show a tetrad morphology, a known feature of *D. radiodurans* cells [23]. If the cell volume is assumed to be filled to a third with a model protein H<sub>50</sub>C<sub>30</sub>N<sub>9</sub>O<sub>10</sub>S<sub>1</sub>, with a density of the cell subunits between 0.5 and 1.1 g/cm<sup>3</sup> [14], the observed phase shift with a maximum value of about 5 rad corresponds to a cell thickness of about 1–2 μm. As expected for soft x-rays, the order of this phase shift exceeds phase changes measured in *D. radiodurans* cells at 6.2 keV, which were in the range of 0.25–0.3 rad [14].

In summary, we have shown that ptychographic data sets on and off resonant with NEXAFS edges allow us to discriminate and to spatially resolve different chemical compositions in amplitude and phase. The phase distribution in the sample provides important chemical information and can be used as a contrast mechanism that is not (or at least not as readily) available in other microscopy techniques (e.g., scanning transmission x-ray microscopy). Even if absorption images at two different energies are similar in contrast (e.g., before and after an absorption

peak) and thus may not provide significant information about the distribution of chemical compounds, the phase shift at those energies might be substantially different. The resolution of the bead reconstructions was estimated to be in the range of one image pixel (96 nm). While the main focus of our experiment was to demonstrate resonant ptychographic CDI, the ultimate goal of wavelength-limited resolution in the soft x-ray range may pose some experimental challenges (some of which have already been discussed in [15]). Also, due to higher wavelengths in the soft x-ray range, the curvature of the Ewald sphere can no longer be neglected if the resolution is increased. At a resolution of roughly 100 nm, however, the Ewald sphere curvature does not need to be taken into account for objects thinner than about  $8.5 \mu\text{m}$  [25].

Images of freeze-dried *D. radiodurans* cells at a photon energy of 517 eV are the first example of a biological specimen imaged by ptychography in the water window. Phase changes of up to 5 rad introduced by the cells are a consequence of the strong interaction of soft x rays with matter. Our results suggest future resonant ptychographic imaging of whole cells, in which changes in phase and amplitude contrast around NEXAFS absorption peaks are predestined to be exploited. The important transition to 3D (tomographic) imaging of biological cells relies on the validity of the projection approximation and the Fourier slice theorem, just as in plane wave CDI or in lens based x-ray microscopy. The different reconstructed exit waves can be identified with the sample projections only if the projection approximation is valid. In other words, diffraction within the sample has to be negligible. While this is also the case for plane wave CDI, the collimated probe in ptychographic CDI may suffer diffraction over the path through the sample even if the sample is very weakly scattering. However, in practical cases the illuminating wave will be more extended than the resolution element, and therefore the depth of focus limitation will be dominated by wavelength and the numerical aperture on the exit side (towards the detector). We hope that this work inspires efforts towards a successful extension of resonant ptychography to unstained, unsliced, vitrified specimens in the water window.

We thank the BESSY II team for help and support during the beam times and M. Grunze for stimulating discussions. The work was funded by the BMBF Grants No. 05KS7VH1 and No. 05K10VH4 (FSP 301-FLASH). Support by the DFG Grant HoloVis (2524/2-1) is kindly acknowledged.

\*beckers@uni-heidelberg.de

†rosenhahn@uni-heidelberg.de

- [1] G. Schneider, *Ultramicroscopy* **75**, 85 (1998).
- [2] J. Miao, P. Charalambous, J. Kirz, and D. Sayre, *Nature (London)* **400**, 342 (1999).
- [3] P. Thibault and V. Elser, *Annu. Rev. Condens. Matter Phys.* **1**, 237 (2010).
- [4] J. Spence, U. Weierstall, and M. Howells, *Ultramicroscopy* **101**, 149 (2004).
- [5] J. Fienup, *Appl. Opt.* **21**, 2758 (1982).
- [6] S. Marchesini, H. He, H. N. Chapman, S. P. Hau-Riege, A. Noy, M. R. Howells, U. Weierstall, and J. C. H. Spence, *Phys. Rev. B* **68**, 140101 (2003).
- [7] H. M. L. Faulkner and J. M. Rodenburg, *Phys. Rev. Lett.* **93**, 23903 (2004).
- [8] J. M. Rodenburg and H. M. L. Faulkner, *Appl. Phys. Lett.* **85**, 4795 (2004).
- [9] P. Thibault, M. Dierolf, A. Menzel, O. Bunk, C. David, and F. Pfeiffer, *Science* **321**, 379 (2008).
- [10] P. Thibault, M. Dierolf, O. Bunk, A. Menzel, and F. Pfeiffer, *Ultramicroscopy* **109**, 338 (2009).
- [11] F. Berenguer de la Cuesta, M. Wenger, R. Bean, L. Bozec, M. Horton, and I. Robinson, *Proc. Natl. Acad. Sci. U.S.A.* **106**, 15 297 (2009).
- [12] M. Dierolf, A. Menzel, P. Thibault, P. Schneider, C. Kewish, R. Wepf, O. Bunk, and F. Pfeiffer, *Nature (London)* **467**, 436 (2010).
- [13] M. Dierolf, P. Thibault, A. Menzel, C. Kewish, K. Jefimovs, I. Schlichting, K. König, O. Bunk, and F. Pfeiffer, *New J. Phys.* **12**, 035017 (2010).
- [14] K. Giewekemeyer, P. Thibault, S. Kalbfleisch, A. Beerlink, C. Kewish, M. Dierolf, F. Pfeiffer, and T. Salditt, *Proc. Natl. Acad. Sci. U.S.A.* **107**, 529 (2010).
- [15] K. Giewekemeyer, M. Beckers, T. Gorniak, M. Grunze, T. Salditt, and A. Rosenhahn, *Opt. Express* **19**, 1037 (2011).
- [16] H. Ade, X. Zhang, S. Cameron, C. Costello, J. Kirz, and S. Williams, *Science* **258**, 972 (1992).
- [17] C. Jacobsen, S. Wirrick, G. Flynn, and C. Zimba, *J. Microsc.* **197**, 173 (2000).
- [18] A. Hitchcock *et al.*, *Ultramicroscopy* **88**, 33 (2001).
- [19] H. Ade and H. Stoll, *Nature Mater.* **8**, 281 (2009).
- [20] C. Song, R. Bergstrom, D. Ramunno-Johnson, H. Jiang, D. Paterson, M. D. de Jonge, I. Mc-Nulty, J. Lee, K. L. Wang, and J. Miao, *Phys. Rev. Lett.* **100**, 025504 (2008).
- [21] T. Beetz and C. Jacobsen, *J. Synchrotron Radiat.* **10**, 280 (2003).
- [22] Y. Yamashita *et al.*, *Phys. Rev. B* **73**, 45336 (2006).
- [23] S. Levin-Zaidman, J. Englander, E. Shimon, A. Sharma, K. Minton, and A. Minsky, *Science* **299**, 254 (2003).
- [24] M. Daly, *Nat. Rev. Microbiol.* **7**, 237 (2009).
- [25] H. Chapman *et al.*, *J. Opt. Soc. Am. A* **23**, 1179 (2006).